



**HAL**  
open science

## Estuarine benthic nitrate reduction rates: Potential role of microalgae?

Anniët M. Laverman, Jérôme Morelle, Céline Roose-Amsaleg, A. Pannard

### ► To cite this version:

Anniët M. Laverman, Jérôme Morelle, Céline Roose-Amsaleg, A. Pannard. Estuarine benthic nitrate reduction rates: Potential role of microalgae?. *Estuarine, Coastal and Shelf Science*, 2021, 257, pp.107394. 10.1016/j.ecss.2021.107394 . hal-03268861

**HAL Id: hal-03268861**

**<https://hal.science/hal-03268861v1>**

Submitted on 28 Jun 2021

**HAL** is a multi-disciplinary open access archive for the deposit and dissemination of scientific research documents, whether they are published or not. The documents may come from teaching and research institutions in France or abroad, or from public or private research centers.

L'archive ouverte pluridisciplinaire **HAL**, est destinée au dépôt et à la diffusion de documents scientifiques de niveau recherche, publiés ou non, émanant des établissements d'enseignement et de recherche français ou étrangers, des laboratoires publics ou privés.

1  
2  
3  
4  
5  
6  
7  
8  
9  
10  
11  
12  
13  
14  
15  
16  
17

# Estuarine benthic nitrate reduction rates: potential role of microalgae?

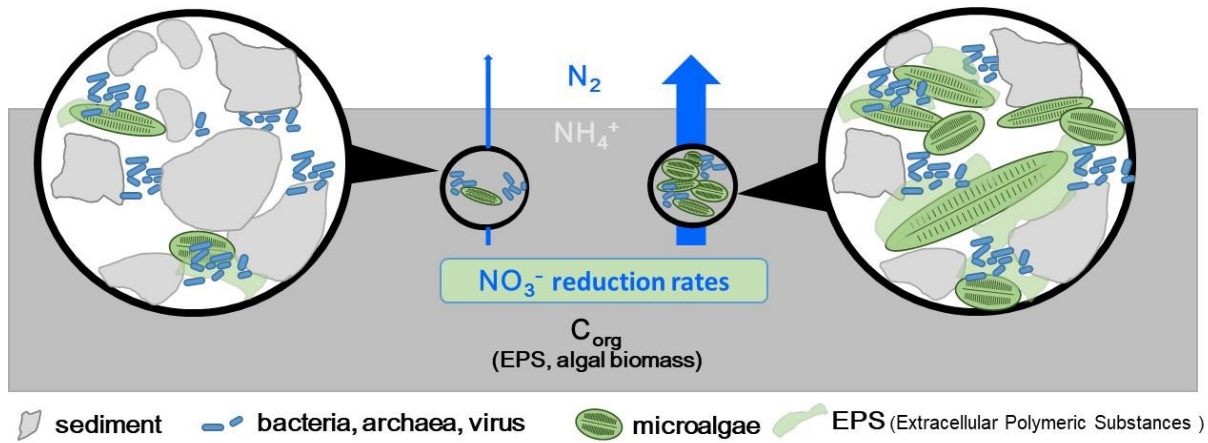
Anniel M. Laverman<sup>1\*</sup>, Jérôme Morelle<sup>1</sup>, Céline Roose-Amsaleg<sup>1</sup>, Alexandrine Pannard<sup>1</sup>

<sup>1</sup>Univ Rennes 1, CNRS, ECOBIO - UMR 6553, F-35000 Rennes, France

\*corresponding author: [anniet.laverman@univ-rennes1.fr](mailto:anniet.laverman@univ-rennes1.fr)

18  
19  
20

Graphical abstract



21  
22  
23

■ sediment    ■ bacteria, archaea, virus    ■ microalgae    ■ EPS (Extracellular Polymeric Substances )

24        **Abstract**

25

26        The ecological functioning of the Seine estuary is strongly affected by the input of nitrogen,  
27 especially in the form of nitrate, which contributes to the eutrophication of the Seine Bight  
28 (France). Elimination of nitrate by benthic denitrification in riparian zones or adjacent wetlands  
29 could significantly improve the water quality of the Seine estuary. The goal of this study was  
30 to investigate the potential for denitrification and the factors affecting these rates. To this end,  
31 we measured nitrate reduction and ammonium production rates using flow-through reactors in  
32 contrasted sediments collected along the Seine Estuary. Sediment and organic carbon  
33 characteristics (organic C, C<sub>org</sub>:N ratio, bioavailable carbon, extracellular polymeric substances  
34 (EPS), chlorophyll *a* and phaeopigments and abundance of nitrogen transforming  
35 microorganisms were determined and related to the potential nitrate reduction rates. Nitrate  
36 reduction rates showed a large spatial and seasonal variation and showed a significant  
37 correlation with sediment phaeopigments, whereas overall microbial activity (ammonium  
38 production rates) were highly correlated to chlorophyll *a* and EPS fractions. Surprisingly,  
39 bacterial abundance was not correlated to nitrate reduction nor to ammonium production rates.  
40 The presence of microalgae appears to be an important driver for nitrate reduction rates in these  
41 riparian sediments and seems to have fueled the benthic nitrate reducing activity.

42

43

44

45        **Key words:** nitrate reduction, organic carbon quality and quantity, microalgae, estuarine  
46 sediments.

47

48

49

50

51

52

## 53 1. Introduction

54 Anthropogenic activity has caused dramatic changes in the global nitrogen cycle. High  
55 loads of nitrogen in streams and rivers due to agricultural activity and waste water treatment  
56 plant effluents are of concern for the coastal zone due to problems associated with  
57 eutrophication (Howarth et al., 1996; Howarth and Marino, 2006). Galloway et al (Galloway et  
58 al., 2004) estimated though that 50% of the nitrogen entering streams and rivers may be  
59 removed before it reaches the coastal waters.

60 In the Seine River basin (France), riparian zones have a high potential of nitrate elimination  
61 (Thouvenot et al., 2007). The amount of nitrogen supplied to the Seine River by agricultural  
62 activity remains high, with little perspective to decrease in the next decades (Garnier et al.,  
63 2019). Recurring eutrophication events in the Seine Bay and other sites in the English Channel,  
64 including harmful algal blooms are thus expected to persist in the future (Garnier et al., 2019).  
65 Therefore, the importance of nitrogen mitigation in the riparian zone is important preventing  
66 eutrophication in the Seine Bight (Cugier et al., 2005). Quantifying and identifying factors  
67 affecting nitrogen transformation processes in the riparian zone of the Seine are thus crucial in  
68 understanding and anticipation of nitrogen elimination.

69 The main process removing excess nitrate from the environment is microbial mediated  
70 denitrification. Denitrification is the microbial respiration of nitrate into reduced nitrogen  
71 species, nitrite, nitrous oxide and dinitrogen gas, while oxidizing organic carbon under anoxic  
72 conditions (Knowles, 1982; Tiedje et al., 1982). Denitrification is usually limited to the top  
73 layers of the sediment where oxygen concentrations are low and nitrate is supplied by the  
74 overlying water. In addition to denitrification, other processes may be responsible for nitrate  
75 reduction. Dissimilatory nitrate reduction to ammonium has been shown to play a role,  
76 transforming nitrate into ammonium, i.e. without any loss of nitrogen from the system (Tiedje,  
77 1988). Anammox, the anaerobic oxidation of nitrate with ammonium, can eliminate oxidized  
78 dissolved nitrogen transforming it into N<sub>2</sub> without requiring the oxidation of organic carbon  
79 (Strous et al., 1999; Vandegraaf et al., 1995).

80 The conditions for denitrification thus require the absence of oxygen, the presence of  
81 nitrate as well as the presence of organic carbon (for review see Tiedje et al., 1982). Numerous  
82 studies have investigated the relation between organic carbon and denitrification rates in soils  
83 and sediments (e.g. Arango et al., 2007; Dodla et al., 2008; Hill and Cardaci, 2004; Sirivedhin  
84 and Gray, 2006). In general, the total amount of organic carbon is a poor predictor for  
85 denitrification rates (Hill and Cardaci, 2004). Some studies demonstrate a significant positive

86 correlation between the amount of total organic carbon and denitrifying capacity (Arango et al.,  
87 2007; Burford and Bremner, 1975), whereas others show no relationship (Gu et al., 2012; Hill  
88 and Cardaci, 2004). This indicates that in addition to the carbon quantity, carbon quality plays  
89 a role in the denitrifying capacity in sediments and soils.

90 Hill and Cardaci (2004) showed that differences in denitrification rates were correlated to  
91 anaerobic mineralizable C contents rather than to the total soil organic carbon content. The  
92 addition of the same quantity of organic carbon to riparian soils resulted in increased  
93 denitrification rates upon watercress and fresh pine needles amendments, whereas significant  
94 lower denitrification rates were measured in the presence of senescent needles (Schipper et al.,  
95 1994). The role of carbon quality was also demonstrated in coastal wetland soils by a positive  
96 correlation of polysaccharide and a negative influence of phenolics on denitrification rates  
97 (Dodla et al., 2008).

98 The impact of carbon quality related to vegetation and its influence on denitrification has  
99 been investigated and suggested in several studies (e.g. Bastviken et al., 2007; Fernandes et al.,  
100 2016; Groffman et al., 1991). Moreover, algal biomass influences denitrification, as shown by  
101 stimulation of denitrification in the presence of senescing green algae (McMillan et al., 2010),  
102 and by the increase of denitrifier abundance upon addition of algal biomass in intertidal  
103 sediments (Decleyre et al., 2015). Both degradation of algal biomass and the presence of  
104 extracellular polymeric substances (EPS) or transparent exopolymeric particles (TEP) secreted  
105 by microalgae (Bohorquez et al., 2017; Passow, 2002; Underwood and Paterson, 2003) might  
106 also be responsible for this increase in denitrifying activity by providing supplementary sources  
107 of anaerobic mineralizable C in sediments. Both terrestrial and aquatic vegetation plays a role  
108 in nitrate reduction *via* the supply of labile and available organic carbon during the degradation  
109 of suspended organic matter (SOM) and consequently nitrate removal in soils and sediments.  
110 Therefore, the objective of this study was to determine the impact of terrestrial and aquatic  
111 vegetation on nitrate reduction rates in riparian estuarine sediments. We hypothesized that  
112 carbon quality rather than carbon quantity drives nitrate reduction rates in these sediments. To  
113 investigate the impact of carbon quality and quantity on nitrate reduction rates, we determined  
114 nitrate reduction rates as well as sediment characteristics in four different estuarine sediments  
115 collected along the Seine River estuary during three different seasons. We used flow-through  
116 reactors to determine the rates under controlled conditions, using intact sediment and thus the  
117 resident microbial community and site specific sediment conditions. In addition to total  
118 sediment organic carbon ( $C_{org}$ ), parameters related to organic carbon quality were determined;

119 the biodegradable organic carbon content (BDOC), %N, C<sub>org</sub>:N ratio, chlorophyll *a* (chl *a*) and  
120 phaeopigments concentrations as well as the EPS fractions (proteins and carbohydrates). In  
121 order to determine whether the bacterial abundances were related to the rates and sediment  
122 characteristics, bacterial abundances as well as those representing the major nitrogen cycling  
123 microbes were enumerated. Nitrate reduction rates were linked to the aforementioned sediment  
124 characteristics and the role of intertidal mudflats mitigating as nitrogen sink is discussed.

125

## 126 **2. Materials and Methods**

127

### 128 **2.1 Study sites and sampling**

129 Surface sediments were collected at 4 sites along the Seine River, France, from just  
130 upstream of Rouen until the estuary mouth (Figure 1). Sediments were collected at low tide  
131 when the sediments were accessible. The most upstream site with near “Saint Etienne du  
132 Rouvray” is a riparian wetland (**RW**, 49°22'12.21"N, 1° 7'13.33"E). It is an old river arm of the  
133 Seine, which is divided in two by an embankment isolating the river the upstream part. The site  
134 corresponds to a closed river arm of the Seine, still connected to the main river and subject to  
135 variations in water levels in relation to the tide. The site is dominated by reed and willow.  
136 “Grand vase petit vase”, near Quevillon (49°25'1.84"N, 0°56'10.45"E), is an artificial wetland  
137 (**AW**) that was created for the deposition of dredging material from the Seine. This so called  
138 “deposit chamber” is connected to the river artificially. At high tide, the site is filled with water  
139 from the Seine River, whereas a valve prevents the water to flow back into the river. “Trou  
140 deshayses” (49°27'22.02"N, 0°51'32.98"E), a freshwater mudflat (**FM**), is a site separated from  
141 the river by a dike with drains containing valves allowing the evacuation of water towards the  
142 river, at the same time preventing inverse flow (from the river to the wetland). This site is fed  
143 by runoff from the alluvial plain and is also influenced by the alluvial groundwater table, main  
144 vegetation is bullrush. The most downstream site, an intertidal mudflat (**IM**), near the village  
145 Petiville (49°25'53.04"N, 0°36'20.87"E), is in direct connection to the Seine River.

146 Nitrate reduction, nitrite and ammonium production rates and sediment characteristics  
147 were determined in June, September 2010 and March 2011. Sediment from the top first cm was  
148 collected for experiments, analysis of sediment characteristics and enumeration of the total  
149 bacterial and denitrifier abundance. Surface water at each sampling site was collected with a 20

150 mL syringe, filtered (0.2  $\mu\text{m}$  pore size) and kept at 4° C during transport (less than 6h) and  
151 frozen until nutrient analysis ( $\text{NO}_3^-$ ,  $\text{NO}_2^-$ ,  $\text{NH}_4^+$ ).

152

153

## 154 **2.2 Flow-through reactor (FTR) experiments**

155 Nitrate reduction as well as nitrite and ammonium production rates were determined in the  
156 top sediment (0-1 cm) using flow-through reactors. The flow-through reactor (FTR) design and  
157 the determination of potential rates were extensively described previously (Laverman et al.,  
158 2006; Pallud et al., 2007; Pallud and Van Cappellen, 2006; Roychoudhury et al., 1998). Upon  
159 collection at low tide, sediments were kept at 4°C until the start of the experiments, which were  
160 started within 24 hours.

161 The sediment in the reactor was supplied with a constant inflow anoxic nitrate solution (5  
162 mM  $\text{NaNO}_3$ ) at ambient salinity (NaCl) at a constant flow rate of  $4.0 \pm 0.2 \text{ mL h}^{-1}$  ( $Q$ ) using a  
163 peristaltic pump (Minipuls 3<sup>®</sup>, Gilson). In these sediments, with a porosity between 0.7 – 0.9  
164 (data not shown), this flowrate has been shown not to influence the potential microbial reaction  
165 rates (Pallud et al., 2007). Note that this flowrate does not mimic *in situ* flowrates. The anoxic  
166 inflow conditions were achieved by bubbling the solutions for 10 minutes with  $\text{N}_2$  gas, kept in  
167 a 1 L Schott bottle closed with a HPLC type cap, to ensure gastight conditions during the  
168 experiment. The HPLC type cap contains an inlet to flush the solution (closed during the  
169 experiment), an outlet that is connected to the peristaltic pump and a pressure in/outlet. The  
170 latter is connected to a syringe filled with  $\text{N}_2$  to compensate possible under pressure during the  
171 experiment and avoiding inflow of air. The reactor outflow solution was sampled at 3 to 4-hour  
172 intervals using a fraction collector over a period of 44 to 50 hours. Reactors were run in  
173 duplicate in June 2010 and March 2011 (44h), which led to 6 samples per reactor at steady state  
174 conditions (20 hours, duplicate reactors  $n=12$ ). In September 2010 triplicate reactors were run  
175 (50h), for FM 1 reactor was clogged and duplicate reactors were taken into account for the rate  
176 determinations, steady state rates were determined upon 14 hours at 3h intervals (36 h,  
177 duplicate  $n=24$ , triplicate  $n=36$ ).

178 Nitrate reduction, nitrite, ammonium production rates were calculated by multiplying the  
179 flow rate,  $Q$ , by the concentration difference of the nitrogen species in the input and output  
180 solutions and normalized to gram dry sediment (see for details Laverman et al 2012). All rates  
181 are expressed in units of nmol per gram dry sediment per hour. Nitrate reduction rates (NRR)  
182 were calculated from the measured difference in nitrate concentration between inflow and



183 outflow solutions. For the nitrite production rates (NiPR) and ammonium production rates  
184 (APR) the inflow concentrations were zero. Note that the rates were determined at constant  
185 temperature ( $20\pm 2^\circ\text{C}$ ) under fully anoxic conditions in the laboratory and are thus referred to  
186 as potential rates. These rates reflect potential rates of the resident microbial community and  
187 sediment organic matter.

188

### 189 **2.3 Analytical methods**

190 Nitrate, nitrite and ammonium concentrations were measured colorimetrically with a  
191 Nutrient Autoanalyzer 3 (Brann and Luebbe, Thermo Scientific). Sediment organic C and total  
192 N contents were determined on freeze-dried samples using a LECO CS 125 CN analyzer. The  
193 sediment samples were acidified drop by drop (100  $\mu\text{L}$ ) with 2N HCl to remove the inorganic  
194 carbon.

195 The amount of biodegradable fraction of the organic carbon (BDOC) in the sediments was  
196 measured using the experimental procedure of Servais et al. (1999). To this end 1  $\text{cm}^3$  of wet  
197 sediment was homogenized in a 1 L bottle with 300 mL deionised water and incubated at  $21\pm 2$   
198  $^\circ\text{C}$ . During incubation the batch was intermittently aerated in order to maintain aerobic  
199 conditions. Subsamples of 40 mL were collected at the beginning and after 45 days of  
200 incubation. They were centrifuged (10 minutes 3000 rpm), the supernatant was transferred to a  
201 glass vial and preserved with 12N HCl (80  $\mu\text{L}$ ) and kept at  $4^\circ\text{C}$  until DOC analysis by high  
202 temperature combustion (Shimadzu TOC-5050A analyzer). The solid pellet was freeze dried,  
203 grinded, acidified and its C content was measured using a total carbon analyzer (LECO CS 125,  
204 EPOC, University Bordeaux 1).

205 Chlorophyll *a* (Chl *a*) and phaeopigments (Phaeo) concentrations in the sediments were  
206 determined according to Lorenzen (1967). The pigments were extracted from 0.5 g of sediment  
207 suspended in 10 mL acetone (90%), by continuously rotating (12 rpm) the samples for 12 h in  
208 the dark at  $4^\circ\text{C}$ . After centrifugation ( $4^\circ\text{C}$ , 2000 g, 5 min), fluorescence of the supernatant was  
209 measured using a Fluorometer Turner TD-700 before and after acidification (10  $\mu\text{L}$  HCl 0.3 M  
210 for 1 mL acetone). Chlorophyll *a* and phaeopigments were then measured using the  
211 fluorometric method (Lorenzen, 1967).

212 Colloidal EPS were extracted from almost 0.5-1 g of dried sediment and placed in 15 mL  
213 centrifugation tubes in 5 mL of deionized water (MilliQ). After 1 h of incubation at  $35^\circ\text{C}$  under  
214 continuous mixing, tubes were centrifuged at  $4^\circ\text{C}$ , 3000 g for 10 min. Supernatants containing  
215 the EPS were collected in a new centrifugation tube. Low and high molecular weight EPS

216 (LMW and HMW) were extracted from the supernatants after incubation in ethanol (70% final  
217 concentration) for 16 h at  $-20^{\circ}\text{C}$ . Samples were centrifuged ( $4^{\circ}\text{C}$ , 3000 g, 30 min). LMW  
218 EPS were collected in the supernatant and HMW EPS were collected in the pellet. The  
219 supernatant was decanted into a new tube and both the supernatant and the pellet were dried at  
220  $60^{\circ}\text{C}$  in a dry bath under air flow (from 6 to 48 h depending on the fraction). The dried samples  
221 were resuspended in 5 mL deionized water and stored at  $-20^{\circ}\text{C}$  for LMW and HMW  
222 carbohydrate and protein quantification. Total sugar content was determined using the phenol–  
223 sulfuric acid assay with glucose as a standard (Dubois et al., 1956) and protein content was  
224 determined using the Bradford assay reagent (Bio-Rad) with bovine serum albumin from  
225 Sigma-Aldrich as standard (Bradford 1976). Absorption was read after 30 min with a  
226 FlexStation plate reader (Molecular Devices) at 485 nm for carbohydrates and 590 nm for  
227 proteins. All results are expressed per gram dry sediment ( $\text{gds}^{-1}$ ).

228  
229

#### 230 **2.4 Microbial abundance measurements**

231 Fresh sediments were collected at the end of the FTR incubation and stored at  $-80^{\circ}\text{C}$  until  
232 DNA extraction. Microbial DNA extraction was carried out according to the protocol described  
233 in (Griffiths et al., 2000). DNA quality and quantity were determined using a Spectrostar nano  
234 (BMG labtech). Quantitative PCRs were conducted with a Roche LC480 thermocycler using  
235 different primer sets targeting several groups of microorganisms. The *nosZ* gene of denitrifying  
236 bacteria (able to transform  $\text{N}_2\text{O}$  in  $\text{N}_2$ ), by using the *nosZ*-F  
237 ( $5'$ -CGYTGTTTCMTGGACAGCCAG, (Kloos et al., 2001) and *nosZ*1622Rb  
238 ( $5'$ -CGCRASGGCAASAAGGTSCG (Throbäck et al., 2004) primer set. The *nrfA* gene for  
239 DNRA (*nrfA*F2aw  $5'$ CARTGYYYGTBGARTA-3', (Welsh et al., 2014) and *nrfA*R1  $5'$ -  
240 WNGGCARTTGRCARTC-3' (Mohan et al., 2004). A region of the *16S rRNA* gene specific to  
241 anammox bacteria (A438F  $5'$ -GTC RGG AGT TAD GAA ATG-3' and A684R  $5'$ -ACC AGA  
242 AGT TCC ACT CTC-3', (Humbert et al., 2012)). The *16S rRNA* gene copies were also  
243 quantified in order to determine a proxy of the whole bacterial density (given that one genome  
244 can contain up to 15 copies of *16S rRNA* genes) using the following primer set: 63f ( $5'$ -  
245 CAGGCCTAACACATGCAAGTC-3' (Marchesi et al., 1998) and BU16S4 ( $5'$ -  
246 CTGCTGCCTCCCGTAGG-3', derived from 341F (Muyzer et al., 1993).

247 Reactions were set up in triplicate; no-template controls in duplicate. Absolute  
248 quantification was performed using 5 serial 10-fold dilutions (in duplicate) using: *Pseudomonas*

249 *fluorescens* SBW25 for *16S rRNA* or gene calibrators from *Escherichia coli* K12 strain for *nrfA*  
250 *gene* and from *Brocadia sp.* (KJ701283) for anammox *16S rRNA gene* and *Bradyrhizobium*  
251 *japonicum* USDA 110 strain for *nosZ* gene.

252 The LC480 software delivered melting curve analysis and second derivatives for crossing  
253 point (Cp) allowing determination of copy numbers. The detection limit was defined as  
254 fluorescent signals with at least 5 Cp below the signal of the no-template controls. All the results  
255 are expressed in log copy numbers per gram dry soil (log copies gds<sup>-1</sup>).

256

## 257 **2.5 Statistical methods**

258 To explain patterns of chemical variability in sediment, the sediment characteristics  
259 determined at the four stations in March, June and September were investigated using a  
260 Principal Component Analysis (PCA), after scaling and reducing the data. All the statistical  
261 analyses were performed using Rstudio (R Core Team 2018), and more specifically, the PCA  
262 was performed using *factoextra* library implemented in R (Kassambara and Mundt, 2017).

263 To highlight factors that best explain the reaction rates in the sediment (Nitrate reduction  
264 NRR, nitrite production NiPR and ammonium production APR), we used a redundancy analysis  
265 (RDA), with a forward selection procedure of the predictors including all chemical variables  
266 (Blanchet et al., 2008). The RDA first performs a multivariate multiple linear regression, then  
267 a PCA of the fitted values, and lastly a permutation test of the significance by randomly  
268 permuting rows and columns. Collinearity between explanatory variables have also been tested.  
269 The RDA was performed using *vegan* and *ade4* libraries in R (Borcard et al., 2011).

270

271

272

### 273 **3. Results**

274

#### 275 **3.1 Site and sediment characteristics**

276 Dissolved nitrogen concentrations in the overlaying water at the sampling sites throughout  
277 the different seasons showed a strong spatial variation. Nitrate was generally the dominant form  
278 of dissolved nitrogen, with highest values in the riparian wetland (70-400  $\mu\text{M}$ ) and values  
279 ranging from 0-105  $\mu\text{M}$  in the artificial wetland, 2-200  $\mu\text{M}$  in the freshwater mudflat and 63-  
280 140  $\mu\text{M}$  in the intertidal mudflat. Ammonium concentrations were high in the riparian wetland  
281 (14-929  $\mu\text{M}$ ), intermediate in the freshwater mudflat (11-60  $\mu\text{M}$ ) and intertidal mudflat (9.3-30  
282  $\mu\text{M}$ ) and low in the artificial mudflat (0.7-4.6  $\mu\text{M}$ ). Nitrate concentrations in the channel of the  
283 Seine River range between 360 to 500  $\mu\text{M}$   $\text{NO}_3^-$  (5 to 7 mg N/L), between 2009 and 2010 at  
284 Poses (Garnier et al 2019).

285

##### 286 **3.1.1 Bacterial abundances**

287 Bacterial abundances were similar (9.2-10.1 log gds<sup>-1</sup>, Table 1) for the total benthic  
288 bacterial community over the different seasons. Denitrifiers represented less than 8% of the  
289 benthic bacteria, bacteria involved in DNRA less than 0.8% and bacteria involved in anammox  
290 0.01% when detectable. The most abundant bacteria able to metabolize nitrate or nitrite were  
291 always the denitrifiers at all sites with the smallest percentages in the artificial wetland and  
292 intertidal mudflat and highest in the riparian wetland and freshwater mudflat (see Table 1)

293

##### 294 **3.1.2 Total and degradable carbon**

295 The total organic carbon contents showed a large variation between the sites and seasons  
296 (Table 2). Lowest organic carbon contents were found for the different seasons in the artificial  
297 wetland and intertidal mudflat sediments, varying between 1.2 and 2.8%. The highest levels of  
298 total organic carbon were found in the sediments of the freshwater mudflat varying between 4.4  
299 and 5.6 % carbon. Relatively high carbon contents were also found in the riparian wetland  
300 sediments, with a large seasonal variation, varying between 2.5-5.7% organic carbon. Most of  
301 the sediment  $\text{C}_{\text{org}}:\text{N}$  ratios are below 11 (Table 2), except high values obtained in the riparian  
302 wetland sediment varying between 31 and 44.

303 The amounts of biodegradable carbon (BDOC) varied between 1 to 13.8 mg C gds<sup>-1</sup> for  
304 the different sampling sites (Table 2). The fractions of BDOC were highest in the freshwater  
305 mudflat and riparian wetland ranging from 6 to 14 mg gds<sup>-1</sup>, lower values were determined for  
306 the artificial wetland (1 – 3.3 mg gds<sup>-1</sup>) and intertidal mudflat (2.4 – 7 mg gds<sup>-1</sup>). The fraction  
307 of biodegradable carbon of the total organic carbon content ranged between 10 to 44% for the  
308 different sediments and showed a high seasonal variation (Table 2). For the riparian wetland  
309 (16–24%), artificial wetland (9-24%) and the freshwater mudflat (10-27%) the values ranged  
310 between 9 and 27%. A larger range of the BDOC fractions was determined in the intertidal  
311 mudflat between 11 and 44% with a high fraction of 44% in March.

312

### 313 **3.1.4 Algae and EPS**

314 Sedimentary chlorophyll *a* and phaeopigment concentrations were highest in the  
315 freshwater mudflat sediments, with concentrations of chl *a* between 21 and 124 µg chl*a* gds<sup>-1</sup>  
316 and phaeopigments ranging from 253 till 611 µg chl*a* gds<sup>-1</sup> (Table 2) The highest values for chl  
317 *a* and phaeopigments did not coincide, chl *a* was highest in March, whereas phaeopigments  
318 were highest in June. Lowest and least variable levels of chl *a* (3.3- 8.5 µg chl*a* gds<sup>-1</sup>) and  
319 phaeopigments (13 – 48 µg eq chl*a* gds<sup>-1</sup>) were measured in the sediments of the riparian  
320 wetland. The artificial wetland and brackish mudflat sediments contained chl *a* and  
321 phaeopigment concentrations between respectively 6.3 to 63 µg chl*a* gds<sup>-1</sup> and 5.3 to 80 µg chl*a*  
322 gds<sup>-1</sup>.

323 The different fractions of the extracellular polymeric substances (EPS) in the different  
324 sediments were dominated by the carbohydrates (ranging between 174 – 313 µg gds<sup>-1</sup>) with  
325 several order of magnitude lower contents of proteins (HMW 0.2 – 8.5 µg gds<sup>-1</sup>; LMW 0.7 – 7  
326 µg gds<sup>-1</sup>). Regarding the total contents of HMW carbohydrates (Table 2), the highest values  
327 were measured in the freshwater mudflat (247-313 µg gds<sup>-1</sup>) while the lowest values were  
328 measured in the intertidal mudflat (174-199 µg gds<sup>-1</sup>). Highest values were measured in June,  
329 except in the artificial wetland. Despite being in the same order of magnitude, LMW  
330 carbohydrates values showed lower variation between sites and seasons. The protein EPS  
331 contents were highest in the freshwater mudflat sediment (HMW 4.5 – 5.8, LMW 4.2 – 7 µg  
332 gds<sup>-1</sup>) and lowest in the riparian wetland sediment (HMW 0.2 – 1.7, LMW 0.7 – 2.3 µg gds<sup>-1</sup>,  
333 see Table 2 for details).

334

### 335 **Correlations**

336 Principal component analysis of the sediment features revealed spatial and temporal  
 337 patterns in the sediment characteristics (Figure 2). The first two principal components (PC1 and  
 338 PC2) explained respectively 51 and 21% of the total variance in the chemical data. The first  
 339 axis was explained by several correlated parameters: the phaeopigment concentrations (Phaeo)  
 340 at 13.6%, the LMW protein fraction of the EPS (prot LMW) and the N content both at 12%, the  
 341 HMW carbohydrate (carb HMW) at 10.4%, the organic carbon ( $C_{org}$ ) and the log-transformed  
 342 denitrifying bacterial numbers (LOGnosZ) both at 9.5% (Fig. 2). The biodegradable carbon  
 343 (BDOC) contents were positively correlated to the  $C_{org}$  content (Spearman correlation,  $r_s=0.68$ ;  
 344  $p = 0.017$ ), while phaeopigments correlated positively with sediment N content ( $r_s=0.87$ ;  $p <$   
 345  $0.001$ ). The second axis was explained by the  $C_{org}$ :N ratio (32%), the BDOC (12.9%), the HMW  
 346 protein fraction of the EPS (prot HMW; 12.5%). The LOGnosZ, which already contributes to  
 347 the first axis, contributes at 9.6% to the second axis. The first axis of the PCA is explained by  
 348 the freshwater mudflat on the left part of the plot, with 31.9%, 22.6% and 16.3% for June,  
 349 September and March samples respectively (Fig. 2). At the opposite side, the March sample  
 350 from the artificial wetland explained 10.6% of the first axis. The second axis of the PCA is  
 351 explained by the March and September samples from the riparian wetland (57.2% and 7.9%  
 352 respectively) at the top of the plot (Figure 2). Finally, the freshwater mudflat showed high  
 353 concentrations of Phaeo,  $C_{org}$ , LMW protein fraction of the EPS, the HMW carbohydrates (carb  
 354 HMW), N and LOGnosZ, whatever the sampling date, while the artificial wetland showed high  
 355  $C_{org}$ :N ratios in March and also in September (Figure 2).

356

357

### 358 **3.2 Nitrate reduction and ammonium production rates**

359 Nitrate reduction rates varied among sites and between seasons (Figure 3, SI Table1).  
 360 Highest nitrate reduction rates were measured in the sediments of the freshwater mudflat,  
 361 especially in June and September with maximum rates up to  $3000 \text{ nmol gds}^{-1} \text{ h}^{-1}$ , with lower  
 362 rates in March (see Figure 3). Overall, the sediments from the different sites showed seasonal  
 363 differences of the potential nitrate reduction rates. Lowest rates were found in March, with  
 364 higher rates in June and September for the sediments from the riparian and artificial wetland  
 365 and brackish mudflat sediments.

366 The ammonium production rates from the same sediments and seasons under nitrate  
 367 reducing conditions, show seasonal variations, however not similar to nitrate reduction rates



368 (Figure 3). The riparian wetland sediment shows low ammonium production rates and little  
369 seasonal variation. The artificial wetland sediment showed highest ammonium production in  
370 March and low rates in June and September, dissimilar to the nitrate reduction rate dynamics.  
371 Highest ammonium production rates were measured from the freshwater mudflat sediments,  
372 the site with highest nitrate reduction rates, in March and June and lowest at this site in  
373 September. The intertidal mudflat sediments showed highest and most variable ammonium  
374 production rates in September and were low in March and June.

375 To highlight which sediment characteristics explain the microbial reaction rates in the  
376 sediment, a redundancy analysis (RDA) was performed on the nitrate reduction rates (NRR),  
377 nitrite production (NiPR) and ammonium production (APR) rates, with a stepwise selection of  
378 explanatory variables (Figure 4). The reaction rates determined using the flow-through reactors  
379 were explained at 83% by four selected parameters, which were the concentrations in both  
380 phaeopigments and in chlorophyll *a*, the HMW carbohydrate and the HMW protein fraction of  
381 the EPS (Figure 4). The first axis of the RDA was correlated with Phaeo (Regression Score  
382 RS=0.98), the HMW carbohydrate fraction (RS=0.82), the HMW protein fraction (RS=0.64)  
383 and the LMW carbohydrate of EPS (RS=0.59). Like the PCA, the first axis separates the  
384 freshwater mudflat (FM) on the right part of the plot, whatever the sampling date, from the  
385 other sites and dates (Figure 4). The second axis of the RDA was mainly correlated with the  
386 LMW carbohydrate of EPS (RS=-0.64), the HMW protein fraction (RS=0.34) and the HMW  
387 carbohydrate of EPS (RS=0.29). The second axis separates samples (except for FM) collected  
388 in September at the bottom part of the plot and samples collected in March (and June for IM)  
389 at the top. The nitrate reduction rate (NRR) is linked to Phaeo and the HMW carbohydrate of  
390 EPS on the RDA (Figure 4), which is confirmed by a correlation between NRR and Phaeo  
391 parameters (Spearman correlation,  $r_s=0.85$ ,  $p<0.001$ ). NRR is also linked to LMW protein  
392 fraction of the EPS, as Phaeo and LMW protein are strongly correlated ( $r_s=0.85$ ;  $p<0.001$ ). In  
393 accordance with correlations observed in the PCA, we also find a correlation between NRR and  
394 N content ( $r=0.72$ ;  $p<0.05$ ). Similarly, in the RDA, ammonium production rate (APR) is linked  
395 to both HMW and LMW carbohydrate of EPS and Phaeo. The intermediate nitrite production  
396 rate (NiPR, data not shown) is more associated with the HMW protein fraction of the EPS and  
397 the LMW carbohydrate of EPS (Figure 4), however these correlations are not significant  
398 ( $r_s=0.34$  and  $r_s=0.42$  respectively;  $p>0.05$ ).

399  
400

401

402 **4. DISCUSSION**

403

404 All sediments adjacent to the Seine River showed a high potential for nitrate reduction.  
405 The role of these sediments as a nitrogen sink is in line with the low nitrate concentrations at  
406 the sampling sites (0-200  $\mu\text{M NO}_3^-$  except one high value of 400  $\mu\text{M NO}_3^-$  at the RW) compared  
407 to concentrations in the Seine river water column (350-500  $\mu\text{M NO}_3^-$ ). In agreement with our  
408 hypothesis, nitrate reduction rates were not correlated to the total organic carbon ( $C_{\text{org}}$ ) quantity  
409 of the sediments. A strong positive correlation was observed between nitrate reduction rates,  
410 phaeopigments and chlorophyll *a*, suggesting a role of freshly degraded algae in nitrate  
411 reduction. The presence of the algae also seems to affect ammonium production rates, strongly  
412 correlated to chl *a* and the carbohydrate and protein EPS fractions, via mineralization of the  
413 algal biomass. The more general indicators for carbon quality, biodegradable carbon fraction  
414 and  $C_{\text{org}}:\text{N}$  ratio, showed neither correlation with nitrate reduction nor ammonium production  
415 rates.

416

417 **4.1 Biodegradable carbon**

418 The degradable organic carbon content in these riparian, estuarine sediments ranged  
419 between 9 and 44 % of the total amount of organic carbon with a strong, significant correlation  
420 between total organic and degradable carbon (Spearman correlation,  $r_s = 0.685$ ,  $p = 0.017$ ).  
421 Similar fractions of biodegradable carbon were determined using the same approach in  
422 suspended matter, between 10 and 25%, in the water column of the Seine River (Servais and  
423 Garnier, 2006) and between 3 and 13 % in intact estuarine sediments under nitrate reducing  
424 conditions in the Scheldt River, Belgium (Abell et al., 2009). The lack of correlation between  
425 the amount of degradable carbon fraction and nitrate reduction rates suggests that this fraction  
426 is a poor indicator for nitrate reduction rates. The measured nitrate reduction rates in this study  
427 were determined on fresh sediment over a relative short period (48 h). The biodegradable  
428 carbon estimation (Servais et al., 1999) is also determined on fresh sediment, under optimal  
429 conditions (i.e. homogenized, aerobic) over a period of 40 days. It is generally considered that  
430 organic matter is made up of an infinite number of fractions with variable degradability,  
431 decreasing over time (Boudreau and Ruddick, 1991). This change over time in carbon  
432 degradability most likely explains the lack of correlation between nitrate reduction rates



433 determined over a short period, degrading the most labile carbon fraction, and the amount of  
434 carbon degraded over a longer time period including a larger range of carbon degradability.

435

436

437

#### 438 **4.2 Nitrate reduction rates related to sediment organic carbon: the role of microalgae.**

439 A strong correlation between the amount of phaeopigments as well as chl $a$  and nitrate  
440 reduction rates suggests an important role of the presence of microalgae. This correlation might  
441 indicate microalgal activity regarding nitrate reduction or consumption; nitrate assimilation by  
442 microphytobenthos (MPB) has been shown to occur and even exceeds denitrification in  
443 estuarine sediments (Sundback and Miles, 2000). This phenomenon is mainly related to low  
444 nitrate availability and photosynthetic conditions. Nitrate can also be stored by diatoms (Kamp  
445 et al., 2011), in vacuoles and used under anoxic conditions. Both assimilation and storage of  
446 nitrate seems unlikely as nitrate reduction rates were determined at high nitrate concentrations  
447 in the dark. The strong correlation of nitrate reduction with phaeopigments, the degraded form  
448 of chl  $a$ , suggests rather the use of dead or senescing algal biomass as a carbon source for nitrate  
449 reduction. This was also shown by a strong increase in nitrate reduction rates upon the addition  
450 of dried algal material (data not shown). This is in agreement with previous studies, showing a  
451 stimulation of denitrification rates by the addition of senescing algal biomass providing N and  
452 labile C to denitrifiers in agricultural headwater stream sediments (McMillan et al., 2010). A  
453 positive correlation was also demonstrated in wetland and pond sediments between  
454 denitrification rates and the presence of diatoms (Ishida et al., 2008). The positive correlation  
455 between nitrate reduction rates and certain fractions of the EPS secreted by MPB indicates a  
456 more indirect effect of the algal presence on nitrate reduction. Nitrate reduction benefits in this  
457 case from EPS that was produced by algae. Exudates of different algal species stimulated  
458 denitrification rates and influenced the denitrifying community structure of periphytic biofilms  
459 (Kalscheur et al., 2012; McMillan et al., 2010). A similar positive effect of EPS, *via* the addition  
460 of MPB biomass, on denitrifier abundance, determined *via* qPCR of *nirS* and *nirK* genes, was  
461 observed in intertidal sediments (Decleyre et al., 2015). It appears that the positive correlation  
462 between the presence of algal biomass and nitrate reduction rates is due to the supply of organic  
463 carbon, either excreted as EPS or the use of algal biomass as a labile carbon source. The addition  
464 of dried algal biomass as carbon source confirms this phenomenon (data not shown).

465 Denitrification can be stimulated by using the extracellular carbon secreted by algae (Wotton  
466 2004) in addition to organic carbon from dead organisms.

467 Despite representing a relative small fraction of the total organic carbon content, the algal  
468 biomass and the EPS carbohydrates are strongly correlated to nitrate reduction rates. A  
469 comparison of the different carbon fractions determined in this study is shown in Table 3. The  
470 amount of algal biomass in carbon units was deduced from the amount of chlorophyll *a* using  
471 a factor of 35  $\mu\text{gC}$  algal biomass per  $\mu\text{g chl}a$  (Garnier et al., 1989), the EPS HMW and LMW  
472 carbohydrates were converted considering the glucose equivalents used in the analysis (Dubois  
473 et al., 1956). The protein fraction, less than 3 % of the EPS fraction, was not considered. The  
474 algal biomass, based on the chlorophyll *a* quantities present in the sediment, made up 0.5 to  
475 5.2% of the total organic carbon fraction. Considering this fraction being biodegradable the  
476 algal biomass would contribute between 2 and 20.5% to the biodegradable carbon in the  
477 different sediments. The algal fraction of total organic carbon as well as the degradable fraction  
478 was lowest (0.5 and 2% respectively) in the riverine wetland sediment, whereas the presence  
479 and contribution to the carbon pools was high at the other sites (3.3-5.2% and 15.1-20.5%).  
480 This is in good agreement with the  $C_{\text{org}}:\text{N}$  ratio (less than 11) of the organic matter indicating  
481 that the origin of organic matter is mainly algal at the AW, FM et IM, whereas the high  $C_{\text{org}}:\text{N}$   
482 ratios at the RW indicates a terrestrial origin (Meyers, 1994).

483 The EPS fraction made up less than 1.5 % of the total organic carbon pool and between  
484 1.8 and 6.3% of the degradable carbon in these sediments. Despite the small variation in total  
485 carbohydrates EPS contents, the contribution of this fraction to the BDOC showed differences  
486 between the sediments; the highest fraction of carbohydrate EPS relative to the amount of  
487 BDOC was found in the artificial wetland sediment, with an average of 6.3%. with lower  
488 proportions in the other sediments (1.8-3.3%).

489

#### 490 ***4.3 Impact of microalgae and their exopolysaccharides secretions on nitrate reduction***

491

492 The strong correlations between phaeopigments and nitrate reduction rates as well as  
493 between the N content and low molecular weight (LMW) proteins as well as high molecular  
494 weight (HMW) carbohydrates suggest a potential role for the EPS fraction as a source of organic  
495 matter in nitrate reduction rates. The LMW compounds are likely the most labile form of EPS  
496 (Welker et al., 2002), which is in good agreement with the positive correlation between the  
497 LMW protein and nitrate reduction rates. The HMW carbohydrates are degraded by

498 exoenzymatic activity into labile LMW compounds (Van Duyl et al 1999), subsequently  
499 available for nitrate reduction.

500 The low molecular weight EPS fraction is continuously secreted by living microalgae  
501 (Orvain et al., 2014) while secretion of high molecular weight EPS is rather controlled by  
502 environmental conditions like irradiance, temperature or salinity (Underwood et al., 2004)  
503 rather to protect cells from dehydration or osmotic shock. The seasonal and spatial presence of  
504 microalgae and the excretion of the different EPS fractions may thus have implications on  
505 nitrate reduction rates in intertidal sediments.

506 Overall, the EPS concentrations showed little seasonal but rather site variation. The protein  
507 fraction was generally low and never exceeded 3% of the carbohydrate fraction, which is in  
508 good agreement with previous observations in intertidal mudflats (Orvain et al., 2014). High  
509 chlorophyll *a* contents in March and/or September in the different sediments are in good  
510 agreement with typical peaks of microalgae biomass in spring and autumn (Kwon et al., 2016).  
511 In general the correlations between the different EPS fractions (LMW and HMW proteins,  
512 HMW carbohydrates) and phaeopigment concentrations and to a lesser extent chlorophyll *a*  
513 link the presence of EPS to the degradation status of the pigments, particularly in summer. The  
514 relative high phaeopigments concentrations, exceeding the chlorophyll *a* contents, reveal the  
515 presence of death algal biomass, being degraded, rather than active production of EPS by the  
516 microalgae in these sediments. The high phaeopigment content, the degradation product of chl*a*,  
517 in summer suggests senescing MPB. This could enhance release of internal EPS into the  
518 environment during MPB cell lysis and/or grazing by benthic fauna (Hubas et al., 2010; van  
519 der Wal et al., 2010), thus becoming available for microbial nitrate reduction during this period.

520 The higher contribution of carbohydrates and proteins in the BDOC in the intertidal  
521 mudflat (5.9-15.6% of BDOC) than in the freshwater mudflat (3.8-9.6% of BDOC) could be  
522 due to a higher secretion of EPS in the intertidal mudflat than in the freshwater mudflat. It has  
523 been shown that EPS secretion protects benthic microalgae against salinity, and prevents drying  
524 of algal cells at low tide (Orvain et al., 2014). The difference in contribution of carbohydrates  
525 and proteins in the BDOC between the riparian wetland (2.9-6.9%) and the artificial wetland  
526 (11.7-41.9%) seems rather due to the higher import of BDOC in the riparian wetland than in  
527 the artificial one. Indeed, the riparian wetland located near the dam of Poses in the upper part  
528 of the estuary, receives relative high DOC quantities from the river (on average  $4 \pm 2.3$  mg  
529 DOC L<sup>-1</sup>) which decrease during the water residence time in the freshwater estuary with a  
530 recycling of organic matter estimated between 40 and 70% (Garnier et al., 2008).

531 The different EPS fractions were related to the measured nitrogen cycling rates. These  
532 associations confirm the potential role of microalgae, *via* their secretions (EPS) in the microbial  
533 degradation and nitrate reduction. Based on these observations and on the results of this study,  
534 the artificial wetland seems to be the location where algae and EPS were the most important as  
535 a support to bacterial denitrification especially in spring (March).

536

537

### 538 **Conclusions**

539 In the investigated sediments, nitrate reduction rates were neither explained by total  
540 organic carbon contents nor the biodegradable carbon fraction. Interestingly a strong positive  
541 correlation between the algal biomass and nitrate reduction indicates a role for microalgae in  
542 benthic nitrate elimination. We hypothesize that the presence of EPS, excreted by microalgae  
543 is the main supplier of organic carbon fueling nitrate reduction. This is in line with the  
544 degradation and incorporation of EPS by heterotrophic bacteria in intertidal sediments  
545 (Bellinger et al., 2009; Taylor et al., 2013). The presence of microalgae at the surface of  
546 intertidal mudflat sediments plays an important role stimulating nitrate reduction and thus the  
547 mitigation of excess nitrate. The excess nitrate has led to coastal eutrophication, with the  
548 occurrence of harmful algal blooms in the Seine Bay (Thorel et al., 2017). In the agricultural  
549 dominated Seine Basin N fluxes remain stable with little perspective of significant decrease,  
550 (Garnier et al., 2019). Our results confirm the role of intertidal mudflats and the presence of  
551 microalgae in biogeochemical nitrogen cycling. Conservation of intertidal mudflats, regarding  
552 the role as nitrogen sink, seems thus important. In the Seine Estuary, undergoing a strong  
553 decrease in the surface of intertidal mudflats (Lesourd et al., 2016), restauration of these areas  
554 might be favorable mitigating nitrogen pollution.

555

### 556 ***Sample CRediT author statement***

557 **Anniët Laverman:** Conceptualization, Methodology, Investigation, Writing- Original  
558 draft preparation, Writing- Reviewing and Editing, Funding acquisition. **Céline Roose-**  
559 **Amsaleg:** Investigation, Writing- Reviewing and Editing. **Jerome Morelle:** Investigation,  
560 Writing- Reviewing and Editing. **Alexandrine Pannard:** Formal analysis, Writing- Reviewing  
561 and Editing.

562

563

564 **ACKNOWLEDGEMENTS**

565 The authors thank Olivier Tronquart, Benjamin Mercier, Simon Decock for nutrient,  
566 BDOC, chlorophyll analysis and assistance in the field; Aurelien Baro for his help with figure  
567 1 and Henri Etcheber for total carbon and nitrogen analysis (EPOC, Bordeaux). This study was  
568 financed by the RE2 Project (SAIV2009-RE2-1) in the GIP Seine-Aval 4 program. Two  
569 anonymous reviewers are acknowledged for their valuable comments on our manuscript.

PREPRINT

570 *References*

571

- 572 Abell, J., Laverman, A.M. and Van Cappellen, P. 2009. Bioavailability of organic matter  
573 in a freshwater estuarine sediment: long-term degradation experiments with and without  
574 nitrate supply. *Biogeochemistry* 94(1), 13-28.
- 575 Arango, C.P., Tank, J.L., Schaller, J.L., Royer, T.V., Bernot, M.J. and David, M.B. 2007.  
576 Benthic organic carbon influences denitrification in streams with high nitrate  
577 concentration. *Freshwater Biology* 52(7), 1210-1222.
- 578 Bastviken, S.K., Eriksson, P.G., Ekstrom, A. and Tonderski, K. 2007. Seasonal  
579 denitrification potential in wetland sediments with organic matter from different plant  
580 species. *Water Air and Soil Pollution* 183(1-4), 25-35.
- 581 Bellinger, B.J., Underwood, G.J.C., Ziegler, S.E. and Gretz, M.R. 2009. Significance of  
582 diatom-derived polymers in carbon flow dynamics within estuarine biofilms determined  
583 through isotopic enrichment. *Aquatic Microbial Ecology* 55(2), 169-187.
- 584 Blanchet, F.G., Legendre, P. and Borcard, D. 2008. Forward selection of explanatory  
585 variables. *Ecology* 89(9), 2623-2632.
- 586 Bohorquez, J., McGenity, T.J., Papaspyrou, S., Garcia-Robledo, E., Corzo, A. and  
587 Underwood, G.J.C. 2017. Different Types of Diatom-Derived Extracellular Polymeric  
588 Substances Drive Changes in Heterotrophic Bacterial Communities from Intertidal  
589 Sediments. *Frontiers in Microbiology* 8, 16.
- 590 Borcard, D., Gillet, F. and Pierre, L. (2011) Numerical ecology with R.
- 591 Boudreau, B.P. and Ruddick, B.R. 1991. On A Reactive Continuum Representation Of  
592 Organic-Matter Diagenesis. *American Journal Of Science* 291(5), 507-538.
- 593 Burford, J.R. and Bremner, J.M. 1975. Relationships between the denitrification  
594 capacities of soils and total, water-soluble and readily decomposable soil organic matter.  
595 7(6), 389.
- 596 Cugier, P., Billen, G., Guillaud, J.F., Garnier, J. and Menesguen, A. 2005. Modelling  
597 the eutrophication of the Seine Bight (France) under historical, present and future  
598 riverine nutrient loading. *Journal Of Hydrology* 304(1-4), 381-396.
- 599 Decleyre, H., Heylen, K., Sabbe, K., Tytgat, B., Deforce, D., Van Nieuwerburgh, F., Van  
600 Colen, C. and Willems, A. 2015. A Doubling of Microphytobenthos Biomass  
601 Coincides with a Tenfold Increase in Denitrifier and Total Bacterial Abundances in  
602 Intertidal Sediments of a Temperate Estuary. *Plos One* 10(5).
- 603 Dodla, S.K., Wang, J.J., DeLaune, R.D. and Cook, R.L. 2008. Denitrification potential  
604 and its relation to organic carbon quality in three coastal wetland soils. *Science of the*  
605 *Total Environment* 407(1), 471-480.
- 606 Dubois, M., Gilles, K.A., Hamilton, J.K., Rebers, P.A. and Smith, F. 1956. Colorimetric  
607 method for the determination of sugars and related substances. *Analytical Chemistry*  
608 28(3), 350-356.
- 609 Fernandes, S.O., Dutta, P., Gonsalves, M.-J., Bonin, P.C. and LokaBharathi, P.A. 2016.  
610 Denitrification activity in mangrove sediments varies with associated vegetation.  
611 *Ecological Engineering* 95, 671-681.
- 612 Galloway, J.N., Dentener, F.J., Capone, D.G., Boyer, E.W., Howarth, R.W., Seitzinger,  
613 S.P., Asner, G.P., Cleveland, C.C., Green, P.A., Holland, E.A., Karl, D.M., Michaels,  
614 A.F., Porter, J.H., Townsend, A.R. and Vorosmarty, C.J. 2004. Nitrogen cycles: past,  
615 present, and future. *Biogeochemistry* 70(2), 153-226.



- 616 Garnier, J., Billen, G., Even, S., Etcheber, H. and Servais, P. 2008. Organic matter  
617 dynamics and budgets in the turbidity maximum zone of the Seine Estuary (France).  
618 *Estuarine Coastal and Shelf Science* 77(1), 150-162.
- 619 Garnier, J., Blanc, P. and Benest, D. 1989. Estimating a carbon chlorophyll ratio in  
620 nanoplankton (Creteil Lake, S-E Paris, France). *Water Resources Bulletin* 25(4), 751-  
621 754.
- 622 Garnier, J., Riou, P., Le Gendre, R., Ramarson, A., Billen, G., Cugier, P., Schapira, M.,  
623 Thery, S., Thieu, V. and Menesguen, A. 2019. Managing the Agri-Food System of  
624 Watersheds to Combat Coastal Eutrophication: A Land-to-Sea Modelling Approach to  
625 the French Coastal English Channel. *Geosciences* 9(10).
- 626 Griffiths, R.I., Whiteley, A.S., O'Donnell, A.G. and Bailey, M.J. 2000. Rapid method  
627 for coextraction of DNA and RNA from natural environments for analysis of ribosomal  
628 DNA- and rRNA-based microbial community composition. *Applied and Environmental*  
629 *Microbiology* 66(12), 5488-5491.
- 630 Groffman, P.M., Axelrod, E.A., Lemunyon, J.L. and Sullivan, W.M. 1991.  
631 Denitrification in grass and forest vegetated filter strips. *Journal of Environmental*  
632 *Quality* 20(3), 671-674.
- 633 Gu, C., Laverman, A.M. and Pallud, C.E. 2012. Environmental controls on nitrogen and  
634 sulfur cycles in surficial aquatic sediments. *Frontiers in Microbiology* 3.
- 635 Hill, A.R. and Cardaci, M. 2004. Denitrification and organic carbon availability in  
636 riparian wetland soils and subsurface sediments. *Soil Science Society of America*  
637 *Journal* 68(1), 320-325.
- 638 Howarth, R.W., Billen, G., Swaney, D., Townsend, A., Jaworski, N., Lajtha, K.,  
639 Downing, J.A., Elmgren, R., Caraco, N., Jordan, T., Berendse, F., Freney, J.,  
640 Kudeyarov, V., Murdoch, P. and Zhu, Z.L. 1996. Regional nitrogen budgets and  
641 riverine N&P fluxes for the drainages to the North Atlantic Ocean: Natural and human  
642 influences. *Biogeochemistry* 35(1), 75-139.
- 643 Howarth, R.W. and Marino, R. 2006. Nitrogen as the limiting nutrient for eutrophication  
644 in coastal marine ecosystems: Evolving views over three decades. *Limnology And*  
645 *Oceanography* 51(1), 364-376.
- 646 Hubas, C., Sachidhanandam, C., Rybarczyk, H., Lubarsky, H.V., Rigaux, A., Moens, T.  
647 and Paterson, D.M. 2010. Bacterivorous nematodes stimulate microbial growth and  
648 exopolymer production in marine sediment microcosms. *Marine Ecology Progress*  
649 *Series* 419, 85-94.
- 650 Humbert, S., Zopfi, J. and Tarnawski, S.-E. 2012. Abundance of anammox bacteria in  
651 different wetland soils. *Environmental Microbiology Reports* 4(5).
- 652 Ishida, C.K., Arnon, S., Peterson, C.G., Kelly, J.J. and Gray, K.A. 2008. Influence of  
653 algal community structure on denitrification rates in periphyton cultivated on artificial  
654 substrata. *Microbial Ecology* 56(1), 140-152.
- 655 Kalscheur, K.N., Rojas, M., Peterson, C.G., Kelly, J.J. and Gray, K.A. 2012. Algal  
656 Exudates and Stream Organic Matter Influence the Structure and Function of  
657 Denitrifying Bacterial Communities. *Microbial Ecology* 64(4), 881-892.
- 658 Kamp, A., de Beer, D., Nitsch, J.L., Lavik, G. and Stief, P. 2011. Diatoms respire nitrate  
659 to survive dark and anoxic conditions. *Proceedings of the National Academy of*  
660 *Sciences of the United States of America* 108(14), 5649-5654.
- 661 Kassambara, A. and Mundt, F. 2017 "Package 'factoextra'." Extract and visualize the  
662 results of multivariate data analyses.
- 663 Kloos, K., Mergel, A., Rosch, C. and Bothe, H. 2001. Denitrification within the genus  
664 *Azospirillum* and other associative bacteria. *Australian Journal Of Plant Physiology*  
665 28(9), 991-998.

- 666 Knowles, R. 1982. Denitrification. *Microbial Reviews* 46(1), 43-70.
- 667 Kwon, B.-O., Lee, Y., Park, J., Ryu, J., Hong, S., Son, S., Lee, S.Y., Nam, J., Koh, C.-H.
- 668 and Khim, J.S. 2016. Temporal dynamics and spatial heterogeneity of microalgal
- 669 biomass in recently reclaimed intertidal flats of the Saemangeum area, Korea. *Journal*
- 670 *of Sea Research* 116, 1-11.
- 671 Laverman, A.M., Van Cappellen, P., van Rotterdam-Los, D., Pallud, C. and Abell, J.
- 672 2006. Potential rates and pathways of microbial nitrate reduction in coastal sediments.
- 673 *FEMS Microbiology Ecology* 58(2), 179-192.
- 674 Lesourd, S., Lesueur, P., Fisson, C. and Dauvin, J.-C. 2016. Sediment evolution in the
- 675 mouth of the Seine estuary (France): A long-term monitoring during the last 150 years.
- 676 *Comptes Rendus Geoscience* 348(6), 442-450.
- 677 Lorenzen, C.J. 1967. Determination of chlorophyll and pheo-pigments -
- 678 spectrophotometric equations. *Limnology and Oceanography* 12(2), 343-&.
- 679 Marchesi, J.R., Sato, T., Weightman, A.J., Martin, T.A., Fry, J.C., Hiom, S.J. and Wade,
- 680 W.G. 1998. Design and evaluation of useful bacterium-specific PCR primers that
- 681 amplify genes coding for bacterial 16S rRNA. *Appl Environ Microbiol* 64(2), 795-799.
- 682 McMillan, S.K., Piehler, M.F., Thompson, S.P. and Paerl, H.W. 2010. Denitrification
- 683 of Nitrogen Released from Senescing Algal Biomass in Coastal Agricultural Headwater
- 684 Streams. *Journal of Environmental Quality* 39(1), 274-281.
- 685 Meyers, P.A. 1994. Preservation of elemental and isotopic source identification of
- 686 sedimentary organic-matter. *Chemical Geology* 114(3-4), 289-302.
- 687 Mohan, S.B., Schmid, M., Jetten, M. and Cole, J. 2004. Detection and widespread
- 688 distribution of the *nrfA* gene encoding nitrite reduction to ammonia, a short circuit in
- 689 the biological nitrogen cycle that competes with denitrification. *Fems Microbiology*
- 690 *Ecology* 49(3), 433-443.
- 691 Muyzer, G., de Waal, E.C. and Uitterlinden, A.G. 1993. Profiling of complex microbial
- 692 populations by denaturing gradient gel electrophoresis analysis of polymerase chain
- 693 reaction-amplified genes coding for 16S rRNA. *Applied and Environmental*
- 694 *Microbiology* 59(3), 695-700.
- 695 Orvain, F., De Crignis, M., Guizien, K., Lefebvre, S., Mallet, C., Takahashi, E. and
- 696 Dupuy, C. 2014. Tidal and seasonal effects on the short-term temporal patterns of
- 697 bacteria, microphytobenthos and exopolymers in natural intertidal biofilms (Brouage,
- 698 France). *Journal of Sea Research* 92, 6-18.
- 699 Pallud, C., Meile, C., Laverman, A.M., Abell, J. and Van Cappellen, P. 2007. The use
- 700 of flow-through sediment reactors in biogeochemical kinetics: Methodology and
- 701 examples of applications. *Marine Chemistry* 106(1-2), 256-271.
- 702 Pallud, C. and Van Cappellen, P. 2006. Kinetics of microbial sulfate reduction in
- 703 estuarine sediments. *Geochimica Et Cosmochimica Acta* 70, 1148-1162.
- 704 Passow, U. 2002. Transparent exopolymer particles (TEP) in aquatic environments.
- 705 *Progress in Oceanography* 55(3-4), 287-333.
- 706 Pignolet, O., Jubeau, S., Vaca-Garcia, C. and Michaud, P. 2013. Highly valuable
- 707 microalgae: biochemical and topological aspects. *Journal of Industrial Microbiology &*
- 708 *Biotechnology* 40(8), 781-796.
- 709 Roychoudhury, A., Viollier, E. and Van Cappellen, P. 1998. A plug flow-through reactor
- 710 for studying biogeochemical reactions in undisturbed aquatic sediments. *Applied*
- 711 *Geochemistry* 13, 269-280.
- 712 Schipper, L.A., Harfoot, C.G., McFarlane, P.N. and Cooper, A.B. 1994. Anaerobic
- 713 decomposition and denitrification during plant decomposition in an organic soil. *Journal*
- 714 *of Environmental Quality* 23(5), 923-928.



- 715 Servais, P. and Garnier, J. 2006. Organic carbon and bacterial heterotrophic activity in  
716 the maximum turbidity zone of the Seine estuary (France). *Aquatic Sciences* 68(1), 78-  
717 85.
- 718 Servais, P., Garnier, J., Demarteau, N., Brion, N. and Billen, G. 1999. Supply of organic  
719 matter and bacteria to aquatic ecosystems through waste water effluents. *Water*  
720 *Research* 33(16), 3521-3531.
- 721 Sirivedhin, T. and Gray, K.A. 2006. Factors affecting denitrification rates in  
722 experimental wetlands: Field and laboratory studies. *Ecological Engineering* 26(2), 167-  
723 181.
- 724 Strous, M., Fuerst, J.A., Kramer, E.H.M., Logemann, S., Muyzer, G., van de Pas-  
725 Schoonen, K.T., Webb, R., Kuenen, J.G. and Jetten, M.S.M. 1999. Missing lithotroph  
726 identified as new planctomycete. *Nature* 400(6743), 446-449.
- 727 Sundback, K. and Miles, A. 2000. Balance between denitrification and microalgal  
728 incorporation of nitrogen in microtidal sediments, NE Kattegat. *Aquatic Microbial*  
729 *Ecology* 22(3), 291-300.
- 730 Taylor, J.D., McKew, B.A., Kuhl, A., McGenity, T.J. and Underwood, G.J.C. 2013.  
731 Microphytobenthic extracellular polymeric substances (EPS) in intertidal sediments  
732 fuel both generalist and specialist EPS-degrading bacteria. *Limnology and*  
733 *Oceanography* 58(4), 1463-1480.
- 734 Thorel, M., Claquin, P., Schapira, M., Le Gendre, R., Riou, P., Goux, D., Le Roy, B.,  
735 Raimbault, V., Deton-Cabanillas, A.-F., Bazin, P., Kientz-Bouchart, V. and Fauchot, J.  
736 2017. Nutrient ratios influence variability in *Pseudo-nitzschia* species diversity and  
737 particulate domoic acid production in the Bay of Seine (France). *Harmful Algae* 68,  
738 192-205.
- 739 Thouvenot, M., Billen, G. and Garnier, J. 2007. Modelling nutrient exchange at the  
740 sediment-water interface of river systems. *Journal of Hydrology* 341(1-2), 55-78.
- 741 Tiedje, J.M. 1988. Ecology of denitrification and dissimilatory nitrate reduction to  
742 ammonium.
- 743 Tiedje, J.M., Sextone, A.J., Myrold, D.D. and Robinson, J.A. 1982. Denitrification:  
744 Ecological niches, competition and survival. *Antonie Van Leeuwenhoek* 48, 569-583.
- 745 Underwood, G.J.C., Boulcott, M., Raines, C.A. and Waldron, K. 2004. Environmental  
746 effects on exopolymer production by marine benthic diatoms: Dynamics, changes in  
747 composition, and pathways of production. *Journal of Phycology* 40(2), 293-304.
- 748 Underwood, G.J.C. and Paterson, D.M. (2003) *Advances in Botanical Research*, Vol 40.  
749 Callow, J.A. (ed), pp. 183-240.
- 750 van der Wal, D., Wielemaker-van den Dool, A. and Herman, P.M.J. 2010. Spatial  
751 Synchrony in Intertidal Benthic Algal Biomass in Temperate Coastal and Estuarine  
752 Ecosystems. *Ecosystems* 13(2), 338-351.
- 753 Vandegraaf, A.A., Mulder, A., Debruijn, P., Jetten, M.S.M., Robertson, L.A. and Kuenen,  
754 J.G. 1995. Anaerobic Oxidation Of Ammonium Is A Biologically Mediated Process.  
755 *Applied And Environmental Microbiology* 61(4), 1246-1251.
- 756 Welsh, A., Chee-Sanford, J.C., Connor, L.M., Loeffler, F.E. and Sanford, R.A. 2014.  
757 Refined *nrfA* Phylogeny Improves PCR-Based *nrfA* Gene Detection. *Applied and*  
758 *Environmental Microbiology* 80(7), 2110-2119.
- 759 Welker, C., Sdrigotti, E., Covelli, S. and Faganeli, J. 2002. Microphytobenthos in the  
760 Gulf of Trieste (Northern Adriatic Sea): Relationship with labile sedimentary organic  
761 matter and nutrients. *Estuarine Coastal and Shelf Science* 55(2), 259-273.
- 762
- 763

## 764 TABLES AND FIGURES

765

766 **Table 1. Bacterial abundance (16S rRNA gene), denitrifying (nosZ gene), DNRA (nrfA gene) and anammox**  
 767 **(amx 16S rRNA gene, "amx") as well as the percentages of the different functional groups of the total bacterial**  
 768 **abundance expressed as gene copie vs 16S determined via qPCR.**

769

Site		LOG 16s (copie gds <sup>-1</sup> )	LOG nosZ	LOG nrfA	LOG amx	nosZ :16s %	Nrf :16s	Amx :16s
RW	March	9.6	8.3	7.2	5.7	4.9	0.4	0.01
	June	9.2	8.0	6.9	5.2	7.2	0.5	0.01
	Sept	9.3	7.9	6.9	5.4	4.4	0.4	0.01
AW	March	9.2	7.5	6.5	b.d.	2.3	0.2	-
	June	9.4	7.7	7.0	b.d.	2.2	0.4	-
	Sept	9.7	8.1	6.8	b.d.	2.6	0.1	-
FM	March	10.1	8.7	7.2	6.1	4.2	0.1	0.01
	June	9.5	8.3	7.4	b.d.	5.6	0.8	-
	Sept	9.5	8.4	7.5	b.d.	6.9	0.8	-
IM	March	9.5	8.1	7.1	5.3	3.6	0.4	0.01
	June	9.3	7.8	6.7	b.d.	3.4	0.3	-
	Sept	9.4	7.9	6.8	b.d.	3.0	0.2	-

770 b.d.: below detection limit

PREPRINT

**Table 2. Characteristics of the sediment at the sampling sites (see figure 1) at the time of sampling. The sediment characteristics include organic carbon ( $C_{org}$ ) and nitrogen (N) content,  $C_{org}$ : N ratio, biodegradable carbon (BDOC), chlorophyll  $a$  (chl  $a$ ), phaeopigments (phaeo), EPS carbohydrates HMW and LMW (carb HMW, carb LMW), EPS proteins (prot HMW and LMW) concentrations.**

Site	Season	$C_{org}$	N	$C_{org}$ :N	BDOC	$BDOC:$ $C_{org}$	chl $a$	phaeo	EPS			
		%		mol :mol	mg gds <sup>-1</sup>	%		carb HMW	carb LMW	prot HMW	prot LMW	
								ug gds <sup>-1</sup>				
RW	March	5.67	0.15	44.1	13.6	24	3.3	13.2	185.3	203.7	0.31	0.69
	June	2.51	0.45	6.5	6.1	24	8.5	47.9	227.7	189.2	0.19	2.33
	Sept	3.68	0.14	30.7	5.8	16	7.5	15.7	187.6	174.2	1.69	1.30
AW	March	1.18	0.24	5.9	1.0	9	6.3	5.3	237.8	177.7	2.58	1.15
	June	1.68	0.36	5.4	3.2	19	5.6	80.3	194.3	187.8	3.27	2.04
	Sept	1.38	0.16	10.4	3.3	24	31.9	42.7	193.9	189.1	2.49	b.d.
FM	March	4.43	0.50	10.4	11.9	27	123.5	253.0	275.0	186.2	4.49	4.22
	June	5.56	0.98	6.7	13.8	25	20.7	611.3	312.6	201.6	5.47	6.99
	Sept	5.63	0.73	9.0	5.7	10	104.7	392.9	246.2	293.4	5.78	4.41
IM	March	1.56	0.18	10.4	6.8	44	7.4	31.5	188.8	205.3	2.58	2.36
	June	2.80	0.45	7.3	4.9	18	15.4	72.8	198.8	190.3	8.45	2.98
	Sept	2.25	0.28	9.5	2.4	11	62.8	63.6	174.2	191.6	2.01	2.79

775

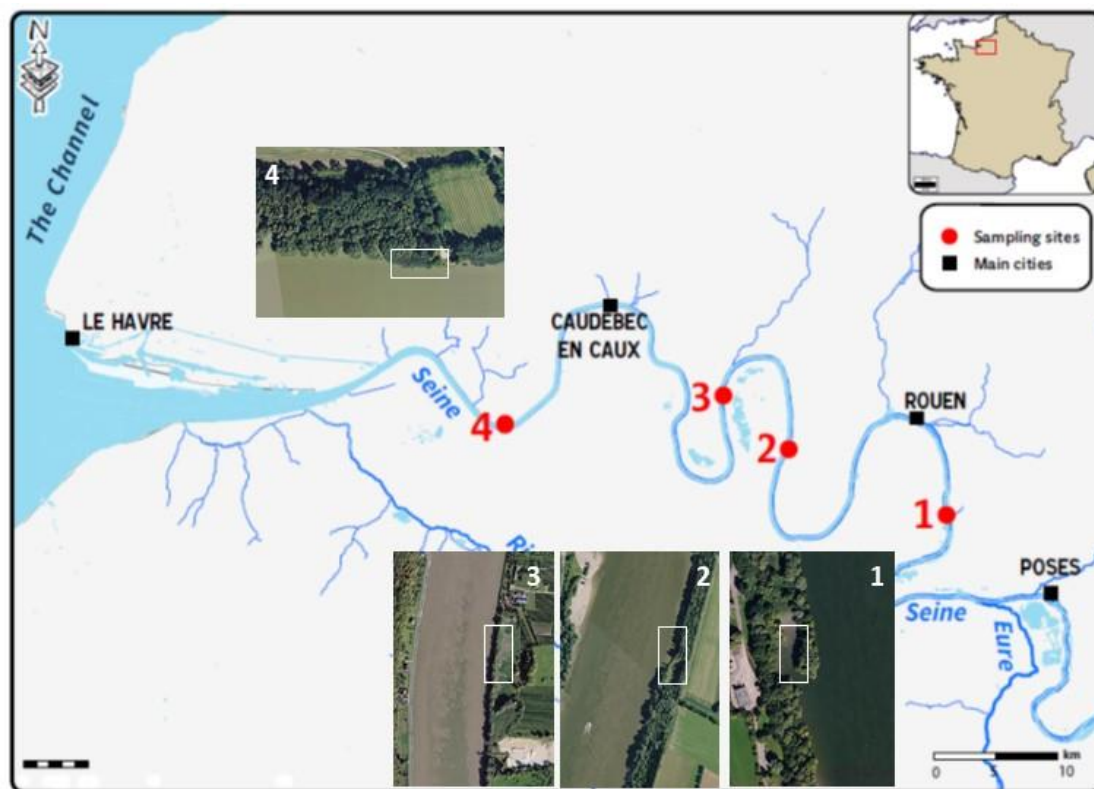
780

**Table 3. The different carbon fractions in the sediments expressed in units C averaged per site. HMW and LMW carbohydrates were converted based on the glucose standard and chlorophyll  $\alpha$  contents were converted with a factor 35 according to Garnier et al (1989).**

site	C <sub>org</sub>	BDOC	algal biomass	EPS	algal biomass: C <sub>org</sub>	algal biomass: BDOC	EPS: C <sub>org</sub>	EPS: BDOC
	mgC gds <sup>-1</sup>				%	%		
RW	31.05	8.48	0.17	0.16	0.5%	2.0%	0.5%	1.8%
AW	11.62	2.51	0.38	0.16	3.3%	15.1%	1.4%	6.3%
FM	41.59	10.48	2.15	0.20	5.2%	20.5%	0.5%	1.9%
IM	17.34	4.70	0.74	0.15	4.3%	15.7%	0.9%	3.3%

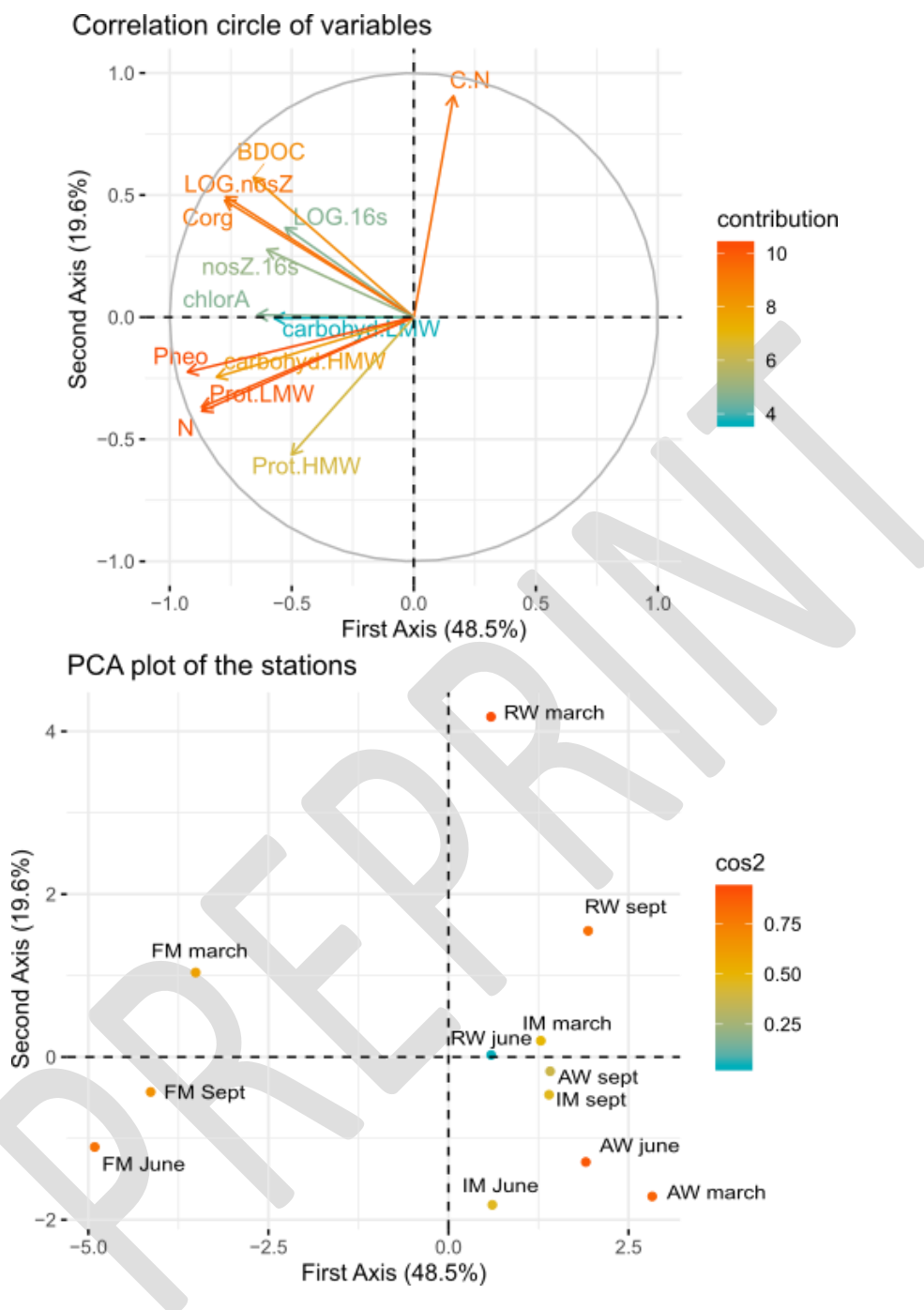
785

790



795

Figure 1. sampling sites from upstream to downstream: (1) riparian wetland RW, (2) artificial wetland AW (3) freshwater mudflat FW and (4) intertidal mudflat IM. The rectangles indicate the locations of the sampling sites. A weir at Poses (upstream of site 1) limits the tidal influence, whereas the upstream limit of saline intrusion is at Caudebex en Caux.



800 **Figure 2.** First two principal axes of the Principal component analysis performed on the sediment  
 characteristics from the sample stations, riverine wetland (RW), artificial wetland (AW), freshwater  
 mudflat (FM) and intertidal mudflat (IM), during the 3 different sampling dates (March, June and  
 805 **September), see section 2.2 for details. Upper right: site scores colored by contribution to axes. Bottom:**  
**factor scores of the variables colored by contribution to axes. The square cosine (square of the correlation**  
**coefficient with PCA axis) gives the quality of the representation of each variable on PCA axis.**

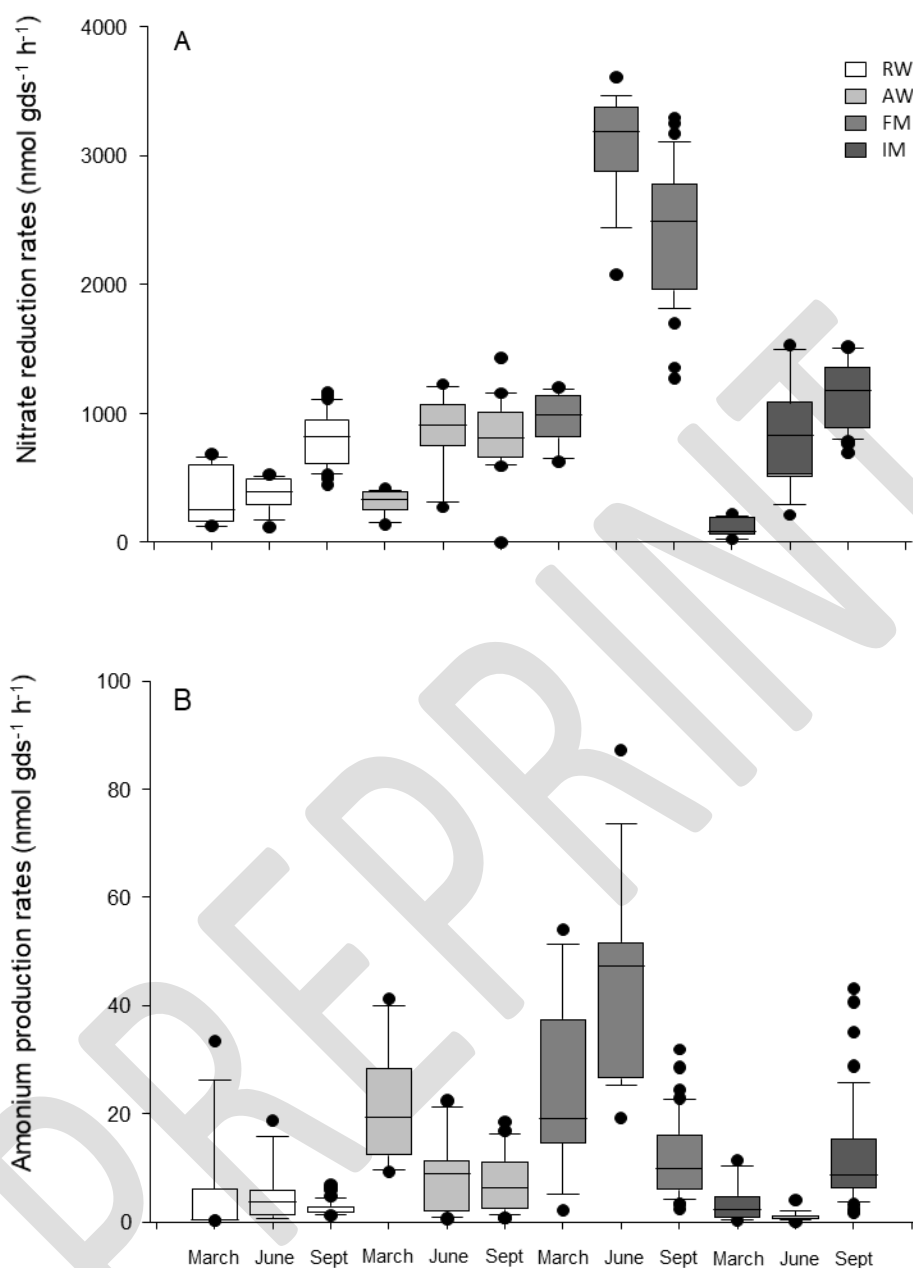
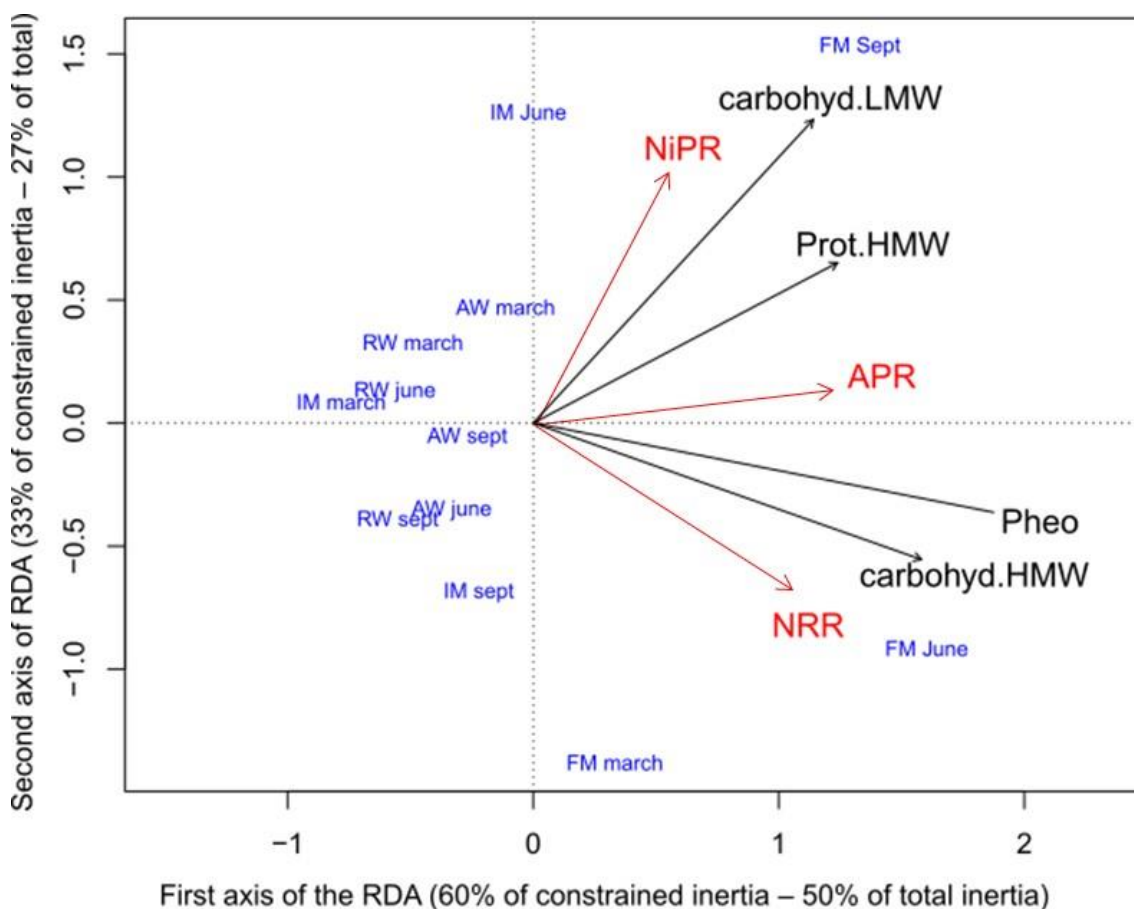


Figure 3. Box plots of the nitrate reduction and ammonium production rates at the 4 sites riverine wetland (RW), artificial wetland (AW), freshwater mudflat (FM) and intertidal mudflat (IM) along the Seine River at the 3 different sampling dates, March (n=12), June (n=12) and September (n=36, except FM n=26), see section 2.2 for details. Boxes encompass the upper and lower quartiles while the line indicates the median, dots are outliers.

810



815

Figure 4. Ordination triplots of the first two axes of the Redundancy Analysis (RDA) between the reaction rates (NRR, NiPR and APR) and the chemical characteristics of the sediment after forward selection (78.9% of constrained variance – 21.1% of residuals). The plot corresponds to the scaling 2, which preserves correlations between descriptors. The reaction rates measured at the different sites, riverine wetland (RW), artificial wetland (AW), freshwater mudflat (FM) and intertidal mudflat (IM), and sampling dates (red vectors) are explained by four chemical parameters selected by the model (blue vectors). Vectors pointing in the same direction indicate a positive correlation, while vectors pointing in opposite direction show a negative correlation. Vectors crossing at right angles indicate independency of both parameters. The absence of collinearity between selected parameters was then checked, as well as the significance of the constrained analysis.

820

825